

Bending analysis of magneto-electro-thermo-elastic functionally graded nano-beam based on first order shear deformation theory

A. Ghorbanpour Arani^{1,*}, A. Hossein Soltan Arani² and E. Haghparast³

^{1,2,3}Faculty of Mechanical Engineering, University of Kashan

Received: 27 February 2018; Accepted: 1 May 2018

ABSTRACT: In this research, analysis of nonlocal magneto-electro-thermo-elastic of a functionally graded nanobeam due to magneto-electro-elastic loads has been done. In order to formulate the problem the Timoshenko theory of beams is utilized. The principle of virtual work, Hamilton's principle as well as nonlocal magneto-electro-thermo-elastic relations has been recruited to derive the governing equations of equilibrium. The small size effect is captured using Eringen's nonlocal elasticity theory. The Electric, Magnetic and Thermal fields are assumed in around of nanobeam. The nanobeam is subjected to transverse loads and initial electric and magnetic potentials. The constitutive relations are used in order to calculate the bending results of the nano-beam for a simply-supported nano-beam in terms of parameters of loadings, materials and geometries. The obtained results in this paper are validated by comparison with existing results in corresponding reference. Remarkable effects such as in-homogeneous parameter, nonlocal parameter, initial electric and magnetic potentials and thermal loads are investigated on the mechanical and electrical results in detail for nanobeams made of METE-FG materials. The results show that with increasing the nonlocal parameter and initial magnetic potentials, deflection of METE-FG nanobeam increases.

Keywords: *Bending; Functionally Graded; In-homogeneous index; Timoshenko theory; Thermo-magneto electrical loads.*

(*) Corresponding Author Email: aghorban@kashanu.ac.ir

INTRODUCTION

Magneto-electro-elastic (MEE) materials are smart materials which possess piezoelectric phase and piezo-magnetic phases. Since the 1970s when the first magneto-electro-elastic composite consisting of the piezomagnetic phase and piezoelectric phase is reported, MEE composite materials are attracted considerable attention. Compared to MEE bulk composite materials, MEE nanomaterials possess higher ME coupling (Lotey and Verma, 2013). Because of converting energy among three forms,

namely electric, magnetic and elastic, MEE materials are widely used in many smart devices, such as sensors, memory devices, actuators, transducers, etc. (Nan, 1994, Huang and Kuo, 1997). (Pan, 2001) derived exact solutions for three-dimensional, anisotropic, linearly MEE, simply-supported, and multilayered rectangular plates under static loadings. Free vibration of MEE beam using in-plane plate, analytically solutions, semi-analytical solutions, approximate solution, finite element approach is carried out by (Vaezi, *et al.*, 2016), (Ramirez, *et al.*, 2006), (Kumaravel, *et al.*, 2007,

Anandkumar, *et al.*, 2007). A new one-dimensional model for the dynamic problem of magneto electro elastic generally laminated beams is presented by (Milazzo, 2013). The electric and magnetic fields are assumed to be quasi-static and a first-order shear beam theory is used. (Reddy, 2007) studied various available beam theories, including the Euler–Bernoulli, Timoshenko, Reddy, and Levinson beam theories, are reformulated using the nonlocal differential constitutive relations of Eringen. He used analytical solutions of bending, vibration and buckling for the nonlocal theories to bring out the effect of the nonlocal behavior on deflections, buckling loads, and natural frequencies. (Ebrahimi and Salari, 2015) by presenting a Navier type solution is investigated the thermal effect on buckling and free vibration characteristics of FG size-dependent Timoshenko nanobeams subjected to thermal loading. Structural elements, such as beams and plates in micro or nano length scale are commonly used as components in micro/nano-electromechanical systems (MEMS/NEMS). (Mohammadimehr, *et al.*, 2016) are presented the free vibration analysis of MEE cylindrical composite panel reinforced by various distributions of carbon nanotubes (CNTs) considering open and closed circuits boundary conditions based on the first order shear deformation theory (FSDT). Study of a dynamic solution for the propagation of harmonic waves in inhomogeneous MEE plates composed of piezoelectric BaTiO₃ and magnetostrictive CoFe₂O₄ are done by (Bin, *et al.*, 2008). They showed that the influential factors of the piezoelectricity and piezomagnetism on the wave characteristics are similar. They utilized the Legendre orthogonal polynomial series expansion approach to determine the wave propagating characteristics in the plates.

Size-dependent nonlinear free vibration (Ansari, *et al.*, 2015a,b), forced vibration in the pre and post buckled (Ansari and Gholami, 2016) of METE nanobeams and nanoplates based upon the nonlocal elasticity theory analyzed by Ansari et al. They used Hamilton's principle for extraction of governing equations which are then discretized via the generalized differential quadrature method (GDQM). Their results demonstrated that the effects of external magnetic potential and electric voltage are dependent on their sign. They found that by increasing temperature nanobeams, the natural frequency of nanobeams slightly decreases while the forced vibration response of these structures is almost insensitive to the temperature rise. It is concluded that increasing nonlocal parameter result in decreasing the total stiffness of METE nanoplate and subsequently lead to the lower values of nondimensional frequencies, for all types of boundary conditions. Using analytical approach, the stress analysis of a long piezoelectric polymeric hollow cylinder reinforced with carbon nanotube (CNT) under combined magneto-thermo-electro-mechanical loading is investigated by (Ghorbanpour arani, *et al.*, 2012). In another work (Ghorbanpour Arani, *et al.*, 2015) studied the stress analysis of composite cylinder reinforced by BNNTs under non-axisymmetric thermo-mechanical loads. Composite materials with inhomogeneous micromechanical structure which are described by the variation in gradually over volume are named Functionally Graded Materials (FGMs). They are composed of two different parts. There are many areas of application for FGM. These materials which are mainly constructed to operate in high temperature environments find their application in nuclear reactors, chemical laboratories, aerospace, turbine

rotors, flywheels and pressure vessels. FGMs have also attracted intensive research interests, which are mainly focused on their bending, vibration, Thermoelastic and buckling characteristics of FGM structures. (Ghorbanpour arani, *et al.*, 2009a,b) analyzed the thermopiezoelectric behavior of a thick walled cylinder with FG materials and to obtain the response of MEE stress and perturbation of the magnetic field vector for a thick walled spherical functionally graded materials (FGM) vessel are developed an analytical method. The classical continuum models need to be extended to consider the nanoscale effects therefore the nonlocal elasticity theory proposed by (Eringen, 1983) which considers the size-dependent effect. Wu and Tsai (2007) developed three-dimensional static behavior of doubly curved MEE-FG shells under the mechanical load, electric displacement and magnetic flux by using an asymptotic approach. Thermo-piezo-magneto-mechanical stresses analysis as well as Semi-analytical solution of magneto-thermo-elastic stresses for functionally graded rotating thin disk is done by (Ghorbanpour arani, *et al.*, 2010a,b). The stress and displacement correlations, including mechanical, magnetic and thermal terms are defined using elasticity theory. It has been found that imposing a magnetic field significantly decreases tensile circumferential stresses. Therefore the fatigue life of the disk will be significantly improved by applying the magnetic field. Free vibration and static analysis of simply supported MEE-FG cylindrical shells and plates analyzed (Bhangale and Ganesan, 2005, 2006). Their results showed that influence of piezoelectric increase the structural frequency marginally and the magnetic effect is reducing the same marginally. Wave propagation analysis of a nanobeam MEE-FG rest on Visco-Pasternak

foundation is developed by (Arefi and Zenkour, 2017). Also in other work (Arefi, 2016) studied the wave propagation in a MEE-FG nano-rod subjected to two-dimensional electric and magnetic potentials. The numerical results indicate that increasing the wave number leads to increasing phase velocity. In two separate work, (Lang and Xuewu, 2013) and (Ebrahimi and Barati, 2016) studied the buckling and vibration of size-dependent METE-FG for circular cylindrical shells and nanosize Beams. They utilized Hamilton's principle and the higher order shear deformation theory for extracting governing equations. In this research because of initial electric and magnetic potentials and thermal loads the size dependent equations of equilibrium for a METE-FG nanobeam is present. Timoshenko beam theories as well as nonlocal magneto-electro-thermo-elastic relations are used to investigate the influence of parameters of materials, geometries and loadings on results of METE-FG nanobeam. In this work an analytical solution for solving the governing equations of motion of bending of a simply supported METE-FG nanobeam is presented. Comparisons with validated references are performed to verify our formulations.

THEORY AND FORMULATION

Contrary to the constitutive equation of classical elasticity theory, Eringen's nonlocal theory (Şimşek and Yurtcu, 2013, Arefi and Zenkour, 2016, Ghorbanpour Arani, *et al.*, 2014, 2018, Eringen, 1972, 1983, 2002) notes that the stress at a reference point is assumed to depend not only on the strain components at this point but is a function of other points stress of the METE body. In this section, the

nonlocalmagneto-electro-thermo-elasticity constitutive relations are expressed.

$$\sigma_{ij} - (e_0 a)^2 \nabla^2 \sigma_{ij} = C_{ijkl} \varepsilon_{kl} - e_{mij} E_m - q_{nij} H_n - \beta_{ij} \Delta T \quad (1)$$

$$D_i - (e_0 a)^2 \nabla^2 D_i = e_{ikl} \varepsilon_{kl} + s_{im} E_m + d_{in} H_n + p_i \Delta T \quad (2)$$

$$B_i - (e_0 a)^2 \nabla^2 B_i = q_{ikl} \varepsilon_{kl} + d_{im} E_m + \chi_{in} H_n + \lambda_i \Delta T \quad (3)$$

In which σ_{ij} , D_i , B_i , E_i and H_i are the stress, electric displacement, magnetic induction, electric field components and magnetic field. C_{ijkl} , e_{mij} , s_{im} , d_{in} , q_{ikl} and χ_{in} are the components of elastic stiffness, piezoelectric, dielectric permittivity constants, magnetoelectric, piezomagnetic and magnetic permittivity constants, respectively, as well as β_{ij} , p_i , λ_i and ρ are the thermal moduli, pyroelectric constants, pyromagnetic constants and mass density, respectively. ΔT is the temperature change and $(e_0 a) \& \nabla^2$ are the scale parameter and the Laplace operator.

$$\sigma_{ij,j} = \rho \ddot{u}_i, \quad D_{i,i} = 0, \quad B_{i,i} = 0 \quad (4)$$

In order to satisfy the Maxwell equations, the electric potential $\phi(x, z, t)$ and the magnetic potential $\psi(x, z, t)$ of METE nanobeams are considered as a combination of a linear and half-cosine variation (Şimşek and Yurtcu, 2013, Arefi and Zenkour, 2016, Ghorbanpour Arani, et al., 2014, 2018, Eringen, 1972, 2002) in which $\xi = \frac{\pi}{h}$,

ψ_0 & ϕ_0 are the initial external magnetic potential and electric potential and, respectively.

$$\Phi(x, z, t) = -\cos(\xi z) \phi(x, t) + \frac{2z}{h} \phi_0 \quad (5)$$

$$\Psi(x, z, t) = -\cos(\xi z) \psi(x, t) + \frac{2z}{h} \psi_0 \quad (6)$$

The non-zero components of magnetic field and electric field using Eqs. (5) and (6) can be expressed

as:

$$E_x = -\frac{\partial \Phi}{\partial x} = \cos(\xi z) \frac{\partial \phi}{\partial x} \quad (7)$$

$$E_z = -\frac{\partial \Phi}{\partial z} = -\xi \sin(\xi z) \phi - \frac{2\phi_0}{h} \quad)$$

$$H_x = -\frac{\partial \Psi}{\partial x} = \cos(\xi z) \frac{\partial \psi}{\partial x} \quad (8)$$

$$H_z = -\frac{\partial \Psi}{\partial z} = -\xi \sin(\xi z) \psi - \frac{2\psi_0}{h} \quad)$$

Timoshenko beam model (TBT)

To model the nanobeam, Timoshenko model of beam is used. Based on this model, two time dependent displacement components along the axial and transverse direction are expressed as:

$$U_1(x, z, t) = u(x, t) + z\theta(x, t) \quad (9)$$

$$U_3(x, z, t) = w(x, t) \quad (10)$$

Where t is time, u and w are displacement components of the mid-plane along x and z directions, respectively. Two components of normal and shear strains using described displacement field in Eqs. (9 – 10), is derived as:

$$\varepsilon_{xx} = \frac{\partial u}{\partial x} + z \frac{\partial \theta}{\partial x}, \quad \gamma_{xz} = \frac{\partial w}{\partial x} + \theta \quad (11)$$

According to Eqs. (1 – 3) and using Eqs. (7,8,11) and Substitution of the required equations, the strain energy of the METE nanobeam is given. Where the bending moment, transverse shear force and normal force are calculated in Eq. 17.

$$U = \frac{1}{2} \int_0^L \int_{-h/2}^{h/2} \left(\sigma_{xx} \varepsilon_{xx} + \sigma_{xz} \gamma_{xz} - D_x E_x \right) dx dz \quad (12)$$

$$\begin{aligned}
 U &= \frac{1}{2} \int_0^L \int_{-h/2}^{h/2} \left(\sigma_{xx} \left(\frac{\partial u}{\partial x} + z \frac{\partial \theta}{\partial x} \right) + \sigma_{xz} \left(\frac{\partial w}{\partial x} + \theta \right) \right) dx dz \\
 &+ \frac{1}{2} \int_0^L \int_{-h/2}^{h/2} \left(B_z \left(\xi \sin(\xi z) \psi + \frac{2\psi_0}{h} \right) \right. \\
 &\quad \left. - B_x \left(\cos(\xi z) \frac{\partial \psi}{\partial x} \right) \right) dx dz \\
 &+ \frac{1}{2} \int_0^L \int_{-h/2}^{h/2} \left(D_z \left(\xi \sin(\xi z) \phi + \frac{2\phi_0}{h} \right) \right. \\
 &\quad \left. - D_x \left(\cos(\xi z) \frac{\partial \phi}{\partial x} \right) \right) dx dz
 \end{aligned} \tag{13}$$

$$\begin{aligned}
 U &= \frac{1}{2} \int_0^L \left(N_x \frac{\partial u}{\partial x} + M_x \frac{\partial \theta}{\partial x} + Q_x \left(\frac{\partial w}{\partial x} + \theta \right) \right) dx \\
 &+ \frac{1}{2} \int_0^L \int_{-h/2}^{h/2} \left(B_z \left(\xi \sin(\xi z) \psi + \frac{2\psi_0}{h} \right) \right. \\
 &\quad \left. - B_x \left(\cos(\xi z) \frac{\partial \psi}{\partial x} \right) \right) dx dz \\
 &+ \frac{1}{2} \int_0^L \int_{-h/2}^{h/2} \left(D_z \left(\xi \sin(\xi z) \phi + \frac{2\phi_0}{h} \right) \right. \\
 &\quad \left. - D_x \left(\cos(\xi z) \frac{\partial \phi}{\partial x} \right) \right) dx dz \\
 (N_x, M_x) &= \int_{-h/2}^{h/2} (1, z) \sigma_{xx} dz, \\
 (Q_x) &= \int_{-h/2}^{h/2} (1) \sigma_{xz} dz
 \end{aligned} \tag{14}$$

The work done by external electric potential, magnetic potential, uniform temperature rise and loading is denoted. In which, N_E, N_H and N_T are the normal force induced by the external electric potential ϕ_0 , external magnetic potential ψ_0 , and temperature rise ΔT .

$$\begin{aligned}
 W &= \frac{1}{2} \int_0^L \left\{ (N_H + N_E + N_T) \left(\frac{\partial w}{\partial x} \right)^2 \right. \\
 &\quad \left. + (qw) \right\} dx \tag{15} \\
 N_H &= - \int_{-h/2}^{h/2} q_{31} \frac{2\psi_0}{h} dz \\
 N_E &= - \int_{-h/2}^{h/2} e_{31} \frac{2\phi_0}{h} dz \tag{16} \\
 N_T &= \int_{-h/2}^{h/2} \beta (T - T_0) dz
 \end{aligned}$$

Now consider the Hamilton's principle, which states that the motion of an elastic structure during the

time interval $t_1 < t < t_2$ is such that the time integral of the total dynamics potential is extreme. Here (U) is strain energy and (W) is work done

$$\int_0^t \delta(U - W) dt = 0 \tag{17}$$

When substituting Eqs. (12–16) into Eq. (17), integrating by parts and setting the coefficients of $\delta u, \delta \theta, \delta w, \delta \phi$ and $\delta \psi$ to zero, the equations of motion will be obtained follows as :

$$\delta u : -\frac{1}{2} \frac{\partial N_x}{\partial x} = 0 \tag{18}$$

$$(N_H + N_E + N_T) \left(\frac{\partial^2 w}{\partial x^2} \right) \tag{19}$$

$$\delta w : -\frac{1}{2} (q) - \frac{1}{2} \frac{\partial Q_x}{\partial x} = 0$$

$$\delta \theta : -\frac{1}{2} \frac{\partial M_x}{\partial x} + \frac{1}{2} Q_x = 0 \tag{20}$$

$$\delta \psi : \frac{1}{2} \int_{-h/2}^{h/2} \left(B_z \xi \sin(\xi z) \right. \\
 \left. + \cos(\xi z) \frac{\partial B_x}{\partial x} \right) dz = 0 \tag{21}$$

$$\delta \phi : \frac{1}{2} \int_{-h/2}^{h/2} \left(D_z \xi \sin(\xi z) \right. \\
 \left. + \cos(\xi z) \frac{\partial D_x}{\partial x} \right) dz = 0 \tag{22}$$

For a magneto-electro-thermo-elastic FGM nanobeam, the nonlocal constitutive relations (1–3) can be approximated to one-dimensional form as:

$$\sigma_{xx} - (e_0 a)^2 \frac{\partial^2 \sigma_{xx}}{\partial x^2} \tag{23}$$

$$= C_{11} \varepsilon_{xx} - e_{31} E_z - q_{31} H_z - \beta_1 \Delta T$$

$$\sigma_{xz} - (e_0 a)^2 \frac{\partial^2 \sigma_{xz}}{\partial x^2} \tag{24}$$

$$= K_s C_{44} \gamma_{xz} - e_{15} E_x - q_{15} H_x$$

$$D_x - (e_0 a)^2 \frac{\partial^2 D_x}{\partial x^2} \tag{25}$$

$$= e_{15} \gamma_{xz} + s_{11} E_x + d_{11} H_x$$

$$D_z - (e_0 a)^2 \frac{\partial^2 D_z}{\partial x^2} \quad (26)$$

$$= e_{31} \varepsilon_{xx} + s_{33} E_z + d_{33} H_z + p_3 \Delta T$$

$$B_x - (e_0 a)^2 \frac{\partial^2 B_x}{\partial x^2} \quad (27)$$

$$= q_{11} \gamma_{xz} + d_{11} E_x + \chi_{11} H_x$$

$$B_z - (e_0 a)^2 \frac{\partial^2 B_z}{\partial x^2} \quad (28)$$

$$= q_{31} \varepsilon_{xx} + d_{33} E_z + \chi_{33} H_z + \lambda_3 \Delta T$$

$K_s = 5/6$ is the shear correction factor (Ebrahimi and Barati, 2016). By substituting Eqs. (23 – 28) into Eqs. (18 – 22), the force-strain and the moment strain of the nonlocal Timoshenko beam theory can be obtained where $\mu = (e_0 a)^2$.

$$N_x - \mu \frac{\partial^2 N_x}{\partial x^2} \quad (29)$$

$$= A_{11} \frac{\partial u}{\partial x} + A_{22} \frac{\partial \theta}{\partial x}$$

$$+ E_{11} \varphi + B_{11} \varphi_0 + Q_{11} \psi + B_{21} \psi_0 - B_{33} \Delta T$$

$$M_x - \mu \frac{\partial^2 M_x}{\partial x^2} \quad (30)$$

$$= A_{22} \frac{\partial u}{\partial x} + A_{33} \frac{\partial \theta}{\partial x}$$

$$+ E_{12} \varphi + B_{12} \varphi_0 + Q_{12} \psi + B_{22} \psi_0 - B_{44} \Delta T$$

$$Q_x - \mu \frac{\partial^2 Q_x}{\partial x^2} \quad (31)$$

$$= K_s A_{12} \frac{\partial w}{\partial x} + K_s A_{12} \theta$$

$$- D_{11} \frac{\partial \varphi}{\partial x} - D_{21} \frac{\partial \psi}{\partial x}$$

$$\int_{-h/2}^{h/2} \left\{ D_x - \mu \frac{\partial^2 D_x}{\partial x^2} \right\} \cos(\xi z) dz \quad (32)$$

$$= D_{11} \frac{\partial w}{\partial x} + D_{11} \theta + T_{11} \frac{\partial \varphi}{\partial x} + T_{12} \frac{\partial \psi}{\partial x}$$

$$\int_{-h/2}^{h/2} \left\{ D_z - \mu \frac{\partial^2 D_z}{\partial x^2} \right\} \xi \sin(\xi z) dz \quad (33)$$

$$= E_{11} \frac{\partial u}{\partial x} + E_{12} \frac{\partial \theta}{\partial x}$$

$$- Y_{11} \varphi - X_{11} \varphi_0 - Y_{12} \psi - X_{12} \psi_0 + Y_{22} \Delta T$$

$$\int_{-h/2}^{h/2} \left\{ B_x - \mu \frac{\partial^2 B_x}{\partial x^2} \right\} \cos(\xi z) dz \quad (34)$$

$$= D_{21} \frac{\partial w}{\partial x} + D_{21} \theta + T_{12} \frac{\partial \varphi}{\partial x} + T_{13} \frac{\partial \psi}{\partial x}$$

$$\int_{-h/2}^{h/2} \left\{ B_z - \mu \frac{\partial^2 B_z}{\partial x^2} \right\} \xi \sin(\xi z) dz \quad (35)$$

$$= Q_{11} \frac{\partial u}{\partial x} + Q_{12} \frac{\partial \theta}{\partial x}$$

$$- Y_{12} \varphi - X_{12} \varphi_0 - Y_{13} \psi - X_{13} \psi_0 + X_{22} \Delta T$$

By substituting Eqs. (18 – 20) into Eqs. (29 – 31), The explicit expressions of the nonlocal normal force, bending moment and shear force can be written.

$$N_x = A_{11} \frac{\partial u}{\partial x} + A_{22} \frac{\partial \theta}{\partial x} \quad (36)$$

$$+ E_{11} \varphi + B_{11} \varphi_0 + Q_{11} \psi + B_{21} \psi_0 - B_{33} \Delta T$$

$$M_x = A_{22} \frac{\partial u}{\partial x} + A_{33} \frac{\partial \theta}{\partial x} + E_{12} \varphi \quad (37)$$

$$+ B_{12} \varphi_0 + Q_{12} \psi + B_{22} \psi_0 - B_{44} \Delta T$$

$$+ 2\mu (N_H + N_E + N_T) \frac{\partial^2 w}{\partial x^2} - \mu q$$

$$Q_x = K_s A_{12} \frac{\partial w}{\partial x} + K_s A_{12} \theta - D_{11} \frac{\partial \varphi}{\partial x} \quad (38)$$

$$- D_{21} \frac{\partial \psi}{\partial x} + 2\mu (N_H + N_E + N_T) \frac{\partial^3 w}{\partial x^3}$$

$$- \mu \frac{\partial q}{\partial x}$$

However, by using Eqs. (18 – 22) and (32 – 38) the governing equation of motion can be re-expressed in the form of u, θ, w, φ and ψ .

$$\delta u: -A_{11} \frac{\partial^2 u}{\partial x^2} - A_{22} \frac{\partial^2 \theta}{\partial x^2} \quad (39)$$

$$- E_{11} \frac{\partial \varphi}{\partial x} - Q_{11} \frac{\partial \psi}{\partial x} = 0$$

$$\begin{aligned} & 2(N_H + N_E + N_T) \frac{\partial^2 w}{\partial x^2} - q - A_{12} \frac{\partial^2 w}{\partial x^2} \\ \delta w : & -A_{12} \frac{\partial \theta}{\partial x} + D_{11} \frac{\partial^2 \varphi}{\partial x^2} + D_{21} \frac{\partial^2 \psi}{\partial x^2} \\ & -2\mu(N_H + N_E + N_T) \frac{\partial^4 w}{\partial x^4} + \mu \frac{\partial^2 q}{\partial x^2} = 0 \end{aligned} \quad (40)$$

$$\begin{aligned} \delta \theta : & A_{12} \frac{\partial w}{\partial x} + A_{12} \theta - D_{11} \frac{\partial \varphi}{\partial x} - D_{21} \frac{\partial \psi}{\partial x} - A_{22} \frac{\partial^2 u}{\partial x^2} \\ & -A_{33} \frac{\partial^2 \theta}{\partial x^2} - E_{12} \frac{\partial \varphi}{\partial x} - Q_{12} \frac{\partial \psi}{\partial x} = 0 \end{aligned} \quad (41)$$

$$\begin{aligned} \delta \psi : & -Y_{13} \psi - X_{13} \psi_0 + X_{22} \Delta T + D_{21} \frac{\partial^2 w}{\partial x^2} \\ & + D_{21} \frac{\partial \theta}{\partial x} + T_{12} \frac{\partial^2 \varphi}{\partial x^2} + T_{13} \frac{\partial^2 \psi}{\partial x^2} = 0 \end{aligned} \quad (42)$$

$$\begin{aligned} \delta \phi : & -Y_{12} \psi - X_{12} \psi_0 + Y_{22} \Delta T + D_{11} \frac{\partial^2 w}{\partial x^2} \\ & + D_{11} \frac{\partial \theta}{\partial x} + T_{11} \frac{\partial^2 \varphi}{\partial x^2} + T_{12} \frac{\partial^2 \psi}{\partial x^2} = 0 \end{aligned} \quad (43)$$

Solution method

In this section, general solution of Eqs. (39–43) as governing equations is presented using complex Fourier series. In this way, to satisfy governing equations of motion, the displacement, rotation and electric and magnetic potential variables are adopted to be of the form: (Ghorbanpour Arani, *et al.*, 2014, Zenkour and Arefi, 2017).

$$u(x, t) = \sum_0^\infty U_n \cos\left(\frac{m\pi}{L} x\right) e^{i\omega_n t} \quad (44)$$

$$\theta(x, t) = \sum_0^\infty \theta_n \cos\left(\frac{m\pi}{L} x\right) e^{i\omega_n t} \quad (45)$$

$$w(x, t) = \sum_0^\infty W_n \sin\left(\frac{m\pi}{L} x\right) e^{i\omega_n t} \quad (46)$$

$$\phi(x, t) = \sum_0^\infty \phi_n \sin\left(\frac{m\pi}{L} x\right) e^{i\omega_n t} \quad (47)$$

$$\psi(x, t) = \sum_0^\infty \psi_n \sin\left(\frac{m\pi}{L} x\right) e^{i\omega_n t} \quad (48)$$

Where $U_n, \theta_n, W_n, \phi_n, \psi_n$ are the coefficients of complex Fourier series represent the amplitudes of the displacement, rotation, the magnetic potential and the electric potential of nanobeams to be determined for each value. Substituting Eq. (44–48) into Eqs. (38–43) leads to Eq. 49 where the elements in the matrixs (K_{ij}, F_{ij}) according to the equations (19–43) are determined.

$$\begin{bmatrix} K_{11} & K_{12} & K_{13} & K_{14} & K_{15} \\ K_{21} & K_{22} & K_{23} & K_{24} & K_{25} \\ K_{31} & K_{32} & K_{33} & K_{34} & K_{35} \\ K_{41} & K_{42} & K_{43} & K_{44} & K_{45} \\ K_{51} & K_{52} & K_{53} & K_{54} & K_{55} \end{bmatrix} \begin{bmatrix} U_n \\ W_n \\ \theta_n \\ \psi_n \\ \phi_n \end{bmatrix} = \begin{bmatrix} F_{11} \\ F_{21} \\ F_{31} \\ F_{41} \\ F_{51} \end{bmatrix} \quad (49)$$

The Material Property

Fig.1 illustrates a METE-FG nanobeam with length L and thickness h exposed to a magnetic potential $\Psi(x, z, t)$, an electric potential $\Phi(x, z, t)$, a uniform temperature rise ΔT and loading $q(x)$.

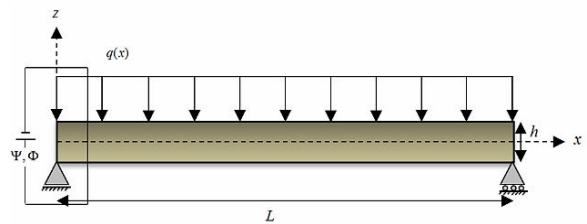


Fig. 1. The schematic configuration of a METE-FG nanobeam

The effective material properties of the METE-FG nanobeam based on power-law form can be displayed in the following form (Şimşek and Yurtcu, 2013):

$$P = P_2 V_2 + P_1 V_1 \quad (50)$$

That P_1 and P_2 are the material properties of the bottom and top surfaces and V_1 and V_2 are the corresponding volume fractions:

$$V_2 + V_1 = 1 \quad V_2 = \left(\frac{z}{h} + \frac{1}{2}\right)^n \quad (51)$$

Where $n \geq 0$ is power index which specifies the material distribution through the thickness of the METE-FG nanobeam. The effective properties of METE-FG nanobeam have been obtained using Eqs. (50–51) with the following form:

$$P(z) = (P_2 - P_1) \left(\frac{z}{h} + \frac{1}{2}\right)^n + P_1 \quad (52)$$

Notice that, the top surface at $z = +h/2$ and the bottom surface $z = -h/2$ of nanobeam are assumed the pure $CoFe_2O_4$ and the pure $BaTiO_3$, respectively. In the Table 1, the values of the METE material properties are expressed (Arefi and Zenkour, 2016, Ghorbanpour Arani, et al., 2018).

The Comparison study

After extensive validation of the present formulation for the elastic nanobeam model by neglecting the piezomagnetic, magnetoelectric and magnetic coefficients $C_{ijkl}, e_{mij}, s_{im}$ and so on, Table 2 are presented for ensuring the accuracy of findings. In which the results of comparison of non-dimensional maximum center deflection $\bar{w} = w * 10^2 (EI/q_0 L^4)$ in simply supported beams subjected to uniform load q_0 (Reddy, 2010) has been displayed.

$$(q_0 = 1, L = 10, E = 30 * 10^6, \nu = 0.3)$$

As can be seen from the Figure, the difference between values is very little, and there is good agreement between two methods.

Table 1. Material properties of $BaTiO_3$ and $CoFe_2O_4$ material.

Parameter	Symbol	$BaTiO_3$	$CoFe_2O_4$
Elastic (Gpa)	C_{11}	166	286
	C_{12}	77	173
	C_{13}	78	170.5
	C_{44}	43	45.3
Piezoelectric (C/m^2)	e_{15}	11.6	0
	e_{31}	-4.4	0
Piezomagnetic (N/Am)	q_{15}	0	550
	q_{31}	0	580.3
Dielectric permittivity ($10^{-9} C/Vm$)	s_{11}	11.2	0.080
	s_{33}	12.6	0.093
Magnetoelectric ($10^{-12} Ns/VC$)	d_{11}	0	0
	d_{33}	0	0
Magnetic permittivity ($10^{-6} Ns^2/C^2$)	χ_{11}	5	-590
	χ_{33}	10	157
Thermal expansion ($10^{-6} 1/K$)	α_x	15.7	10
	α_y	15.7	10
	α_z	6.4	10
Pyromagnetic ($10^{-6} N/AmK$)	λ_3	5.187	5.187
Pyroelectric $10^{-6} (C/N)$	p_3	-2.94	25
Mass density (Kg/m^3)	ρ	5850	5300
* $\beta = C_{11}\alpha_x + C_{12}\alpha_y + C_{13}\alpha_z$			

Table 2. Comparison of non-dimensional maximum center deflection (Reddy, 2010).

TBT (PRE)	TBT (REF)	EBT (REF)	μ	L/h
1.3074	1.3134	1.3130	0	100
1.3720	1.3813	1.3809	0.5	
1.4365	1.4492	1.4487	1	
1.5010	1.5170	1.5165	1.5	
1.5655	1.5849	1.5844	2	
1.3155	1.3218	1.3130	0	20
1.3804	1.3909	1.3809	0.5	
1.4453	1.4600	1.4487	1	
1.5102	1.5290	1.5165	1.5	
1.5752	1.5981	1.5844	2	
1.3406	1.3483	1.3130	0	10
1.4068	1.4210	1.3809	0.5	
1.4730	1.4937	1.4487	1	
1.5391	1.5664	1.5165	1.5	
1.6053	1.6391	1.5844	2	

RESULTS AND DISCUSSION

As can be seen, Fig. 2 depicts the variations of dimensionless transverse deflection $1000*(w/L)$ versus nonlocal parameters of METE-FG nanobeam ($m = 1, \psi_0 = \phi_0 = \Delta T = 0$) for various shear effect coefficient. From this Figure is taken that by increasing nonlocal parameters, the dimensionless deflection of nanobeam increases. As well as considering the shear effect coefficient, the ratio $1000*(w/L)$ increases. Increase of non-dimensional deflection of nanobeam is due to decrease of stiffness of nanobeam with increase of nonlocal parameters. The influence of initial magnetic potentials of METE-FG nanobeam on the

variation of non-dimensional deflection $1000*(w/L)$ of nanobeam ($m = 1, \mu = 1, \phi_0 = 1, \Delta T = 0$) is presented in Fig. 3. The numerical results indicate that the absolute value of non-dimensional deflection $1000*(w/L)$ of nanobeam is increased with increase of initial magnetic potential and also decrease of initial inhomogeneous index. This event has been created due to material properties changes of the nanobeam.

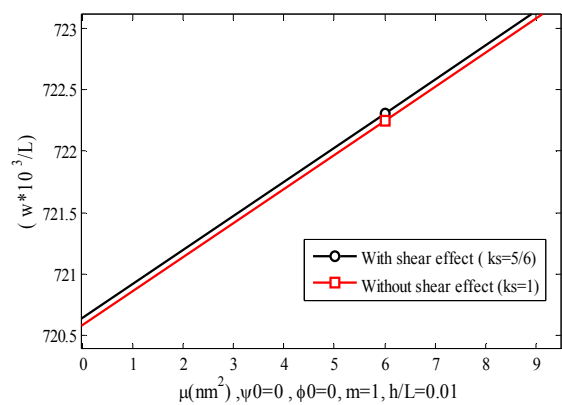


Fig. 2. Variations of dimensionless transverse deflection versus nonlocal parameters of METE-FG nanobeam for various shear effect ($m = 1, \psi_0 = \phi_0 = \Delta T = 0$)

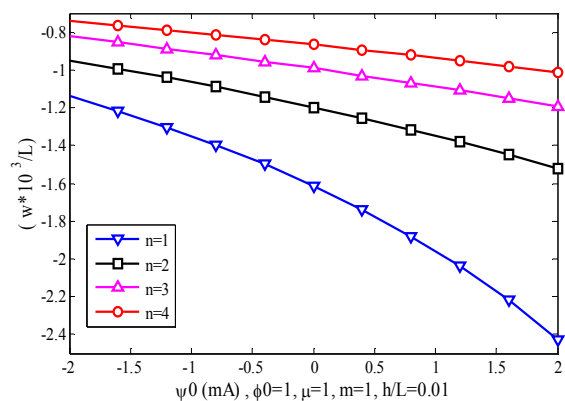


Fig. 3. Variations of dimensionless transverse deflection versus initial magnetic potentials of METE-FG nanobeam for various in-homogeneous index ($m = 1, \mu = 1, \phi_0 = 1, \Delta T = 0$)

Fig. 4 displays that non-dimensional deflection $1000*(w/L)$ versus nonlocal parameters of METE-FG nanobeam for various in-homogeneous index ($m=1, \psi_0 = \phi_0 = \Delta T = 0$). It is understood that with increasing the nonlocal parameter and in-homogeneous index, the dimensionless transverse deflection increases. This is due to decrease of stiffness of METE-FG nanobeam.

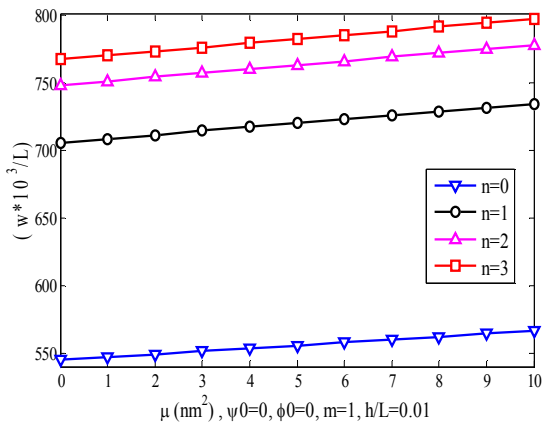


Fig. 4. Variations of dimensionless transverse deflection versus nonlocal parameters of METE-FG nanobeam for various in-homogeneous index ($m=1, \psi_0 = \phi_0 = \Delta T = 0$)

The variation of non-dimensional deflection $1000*(w/L)$ in terms of temperature rising and inhomogeneous index ($m=1, \mu=1, \psi_0 = \phi_0 = 0$) is demonstrated in Fig. 5. It shows that with increase of in-homogeneous index and also decrease of temperature rising, the non-dimensional deflection $1000*(w/L)$ increases. The effects of variations of dimensionless transverse deflection for various inhomogeneous indexes of METE-FG nanobeam versus initial electric potentials ($m=1, \mu=1, \psi_0 = \Delta T = 0$) are illustrated in Fig. 6.

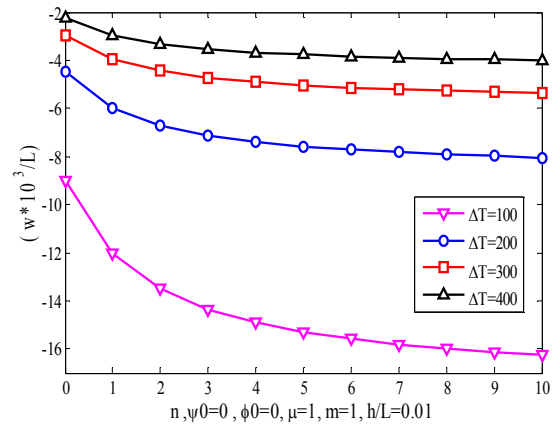


Fig. 5. The effect of temperature rising on dimensionless transverse deflection of METE-FG nanobeam versus on in-homogeneous index ($m=1, \mu=1, \psi_0 = \phi_0 = 0$)

According to Fig. 6, increasing initial electric potentials lead to decrease the dimensionless transverse deflection. Also, this Figure demonstrates that increasing in-homogeneous reduces the stiffness of the beam in result non-dimensional deflection $1000*(w/L)$ increases.

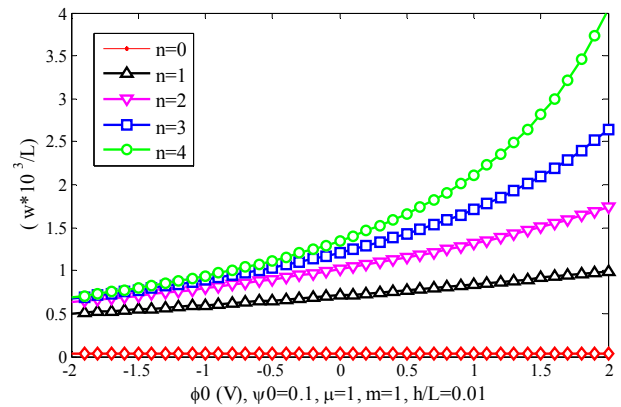


Fig. 6. Variations of dimensionless transverse deflection for various in-homogeneous index of METE-FG nanobeam versus initial electric potentials ($m=1, \mu=1, \psi_0 = \Delta T = 0$)

Fig.7 indicates that change of non-dimensional deflection $1000*(w/L)$ of nanobeam in terms of thickness to length ratio h/L for various inhomogeneous indexes.

$$(m = 1, \mu = 1, \psi_0 = \phi_0 = \Delta T = 0)$$

This Figure illustrates that with increase of thickness-to-length ratio h/L , the non-dimensional deflection of nanobeam is decreased significantly. In addition, from this Figure can be concluded that results converges for higher values of h/L . Decrease of non-dimensional deflection of nanobeam is due to increase of stiffness of nanobeam with increase of h/L .

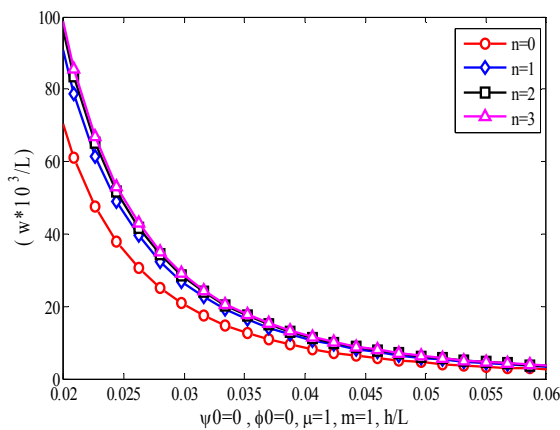


Fig. 7. The effect of different in-homogeneous index on dimensionless transverse deflection of METE-FG nanobeam versus thickness-to-length ratio ($m = 1, \mu = 1, \psi_0 = \phi_0 = \Delta T = 0$)

CONCLUSIONS

In this paper, an analytically solutions for a functionally graded nanobeam is developed. The nanobeam made of magneto-electro-thermo-elastic material. The nonlocal magneto-electro-thermo-elastic relations as well as principle of virtual work are employed for formulation of the problem. The nanobeam is subjected to transverse loads and magneto-electro-thermal loads. Timoshenko beam theory considering the shear correction factor is utilized for description of displacement field. In addition electric and magnetic potentials are

presented in the form of a linear distribution and a cosine distribution to mention initial electric and magnetic potentials. The governing equations of equilibrium are derived using the elasticity theory by assuming power functions for all mechanical, electrical, magnetical and thermal properties. The used analytical solution is based on Fourier series where numerical analysis of the problem and investigation on the influence of important parameters of the problem is solved by it.

The important parameters of the problem are divided to parameters of loads, geometries and materials. Subsequently, the influences of the in-homogeneous parameter, nonlocal parameter, initial electric and magnetic potentials and thermal loads are investigated on the mechanical and electrical results in detail for nanobeams made of METE-FG materials. The numerical results lead to important conclusions as follows:

1. Change of initial electric and magnetic potentials can change the bending and electromagnetic behaviors of nanobeam. The results demonstrates that by increasing initial electric potential and initial magnetic potential, the maximum of non-dimensional deflection increase.
2. Nonlocal parameter of nanomaterials can strongly change the results of the problem. This study shows that increase of nonlocal parameter leads to increase transverse deflections. Also from these results are understood that increases of transverse displacements by increasing of in-homogeneous index.
3. Temperature rising of METE-FG nanobeam leads decrease transverse displacements.
4. The parameter thickness-to-length ratio h/L has important effect on the results of the problem. By increasing of this parameter leads to

decrease and converges of non-dimensional transverse displacement.

5. The shear correction factor is another effective parameter. This parameter has a small incremental effect on the bending behavior of METE-FG nanobeam.

REFERENCES

- Lotey, G.S.; Verma, N. (2013). Magnetolectric coupling in multiferroic BiFeO₃ nanowires. *Chem. Phys. Lett.*, 579: 78-84.
- Nan, C.W. (1994). Magneto electric effect in composites of piezoelectric and piezomagnetic phases. *Phys. Rev. B*, 50: 6082–6088.
- Huang, J.H.; Kuo, W.S. (1997). The analysis of piezoelectric/piezomagnetic composite materials containing ellipsoidal inclusions. *J. Appl. Phys.*, 8: 1378–1386.
- Pan, E. (2001). Exact Solution for Simply Supported and Multilayered Magneto-Electro Elastic Plates. *J Appl. Mech.*, 68(4): 608-618.
- Anandkumar, R.A.; Ganesan, N.; Swarnamani, S. (2000). Free vibration behavior of multiphase and layered magneto-electro-elastic beam. *J Sound Vib*, 299: 44 – 63.
- Kumaravel, A.; Ganesan, N.; Sethuraman, R. (2007). Buckling and vibration analysis of layered and multiphase magneto-electro-elastic beam under thermal environment. *Multidiscipline Modeling in Mat. and Str.*, 3 (4): 461-476.
- Ramirez, F.; Heyliger, P.R.; Pan, E. (2006). Free vibration response of two-dimensional magneto-electro-elastic laminated plates. *J Sound Vib*, 292: 626- 644.
- Vaezi, M.; Moory Shirbani, M.; Hajnayeb, A. (2016). Free vibration analysis of magneto-electro-elastic microbeams subjected to magneto-electric loads. *Physica E*, 75: 280–286.
- Milazzo, A. (2013). A one-dimensional model for dynamic analysis of generally layered magneto-electro-elastic beams. *J Sound Vib*, 332:465–483.
- Reddy, J.N. (2007). Nonlocal theories for bending, buckling and vibration of beams. *Int. J Eng. Sci.*, 45: 288–307.
- Ebrahimi, F.; Salari, E. (2015). Thermal buckling and free vibration analysis of size dependent Timoshenko FG nanobeams in thermal environments. *Composite Structures*, 128: 363–380.
- Mohammadimehr, M.; Okhravi, S.V.; Akhavan Alavi, S.M. (2016). Free vibration analysis of magneto-electro-elastic cylindrical composite panel reinforced by various distributions of CNTs with considering open and closed circuits boundary conditions based on FSDT. *J Vib Control*, 288: 412–422.
- Bin, W.; Jiangong, Y.; Cunfu, H. (2008). Wave propagation in non-homogeneous magneto-electro-elastic plates. *J Sound Vib*, 317: 250- 264.
- Ansari, R.; Gholami, R.; Rouhi, H. (2015a). Size-Dependent Nonlinear Forced Vibration Analysis of Magneto-Electro-Thermo-Elastic Timoshenko Nanobeams Based upon the Nonlocal Elasticity Theory. *Compos Struct*, 126: 216-226.
- Ansari, R.; Hasrati, E.; Gholami, R.; Sadeghi, F. (2015b). Nonlinear analysis of forced vibration of nonlocal third-order shear deformable beam model of magneto-electro-thermo elastic nanobeams. *Composites Part B*, 83: 226-241.
- Ansari, R.; Gholami, R. (2016). Nonlocal free vibration in the pre and post buckled states of magneto-electro-thermo elastic rectangular nanoplates with various edge conditions. *Smart Mater. Struct*, 25: 095033.
- Ghorbanpour Arani, A.; Mobarakeh, M. R.; Shams, S.; Mohammadimehr, M. (2012). The effect of CNT volume fraction on the magneto-thermo-electro-

- mechanical behavior of smart nanocomposite cylinder. *J Mech. Sci. Technol*, 26(8): 2565-2572.
- Ghorbanpour Arani, A.; Haghparast, E.; Khoddami Maraghi, Z.; Amir, S. (2015). Exact Solution for Electro-Thermo-Mechanical Behavior of Composite Cylinder Reinforced by BNNTs under Non-Axisymmetric Thermo-Mechanical Loads. *AUT J Model Simul.*, 45(1): 15-25.
- Ghorbanpour Arani A.; Khoshgoftar, M. J.; Arefi, M.; (2009a). Thermoelastic analysis of a thick walled cylinder made of functionally graded piezoelectric material. *Smart Mater Struct*, 18 (11): 5007.
- Ghorbanpour Arani, A.; Salari, Khademizadeh, H.; Arefmanesh, A. (2009b). Magneto-thermoelastic transient response of a functionally graded thick hollow sphere subjected to magnetic and thermoelastic fields. *Arch Appl. Mech.*, 79: 481–497.
- Eringen, A.C. (1983). On differential equations of nonlocal elasticity and solutions of screw dislocation and surface waves. *J. Appl. Phys.*, 54: 4703-4710.
- Wu, C.P.; Tsai, Y.H. (2007). Static behavior of functionally graded magneto-electro-elastic shells under electric displacement and magnetic flux. *Int. J Eng. Sci.*, 45: 744–769.
- Ghorbanpour Arani, A.; Loghman, A.; Shajari, A.R.; Amir, S. (2010a). Semi-analytical solution of magneto-thermo-elastic stresses for functionally graded variable thickness rotating disks. *J Mech. Sci. Technol.*, 24 (10): 2107-2118.
- Ghorbanpour Arani, A.; Maraghi, Z.K.; Mozdianfard, M.R.; Shajari, A.R. (2010b). Thermo-piezo-magneto-mechanical stresses analysis of FGPM hollow rotating thin disk. *Int. J Mech. Mater. Des.*, 6(4): 341-349.
- Bhangale, R.K.; Ganesan, N. (2005). Free vibration studies of simply supported non-homogeneous functionally graded magneto-electro-elastic finite cylindrical shells. *J Sound Vib*, 288: 412- 422.
- Bhangale, R.K.; Ganesan, N. (2006). Static analysis of simply supported functionally graded and layered magneto-electro-elastic plates. *Int J Solids Struct*, 43: 3230–3253.
- Arefi, M.; Zenkour, A.M. (2017). Wave propagation analysis of a functionally graded magneto-electro-elastic nanobeam rest on visco-Pasternak foundation. *Mech Res. Commun*, 79: 51-62.
- Arefi, M. (2016). Analysis of wave in a functionally graded magneto-electroelastic nano-rod using nonlocal elasticity model subjected to electric and magnetic potentials. *Acta Mech*, 227 (9): 2529–2542.
- Lang, Zh.; Xuewu, L. (2013). Buckling and vibration analysis of functionally graded magneto-electro-thermo-elastic circular cylindrical shells. *Appl Math Model*, 37: 2279–2292.
- Ebrahimi, F.; Barati, M.R. (2016). Buckling Analysis of Smart Size-Dependent Higher Order Magneto-Electro-Thermo-Elastic Functionally Graded Nanosize Beams. *J Mech*, 33 (01): 23-33.
- Şimşek, M.; Yurtcu, H.H. (2013). Analytical solutions for bending and buckling of functionally graded nanobeams -386.
- Arefi, M.; Zenkour, A.M. (2016). Employing sinusoidal shear deformation plate theory for transient analysis of three layers sandwich nanoplate integrated with piezo-magnetic face-sheets, *Smart Mater. Struct*, 25 (11): 115040-57.
- Ghorbanpour Arani, A.; BabaAkbar Zarei, H.; Haghparast, E. (2018). Vibration response of viscoelastic sandwich plate with magnetorheological fluid core and functionally graded-piezoelectric nanocomposite face sheets. *J Vib. Control*, 1-17.
- Eringen, A.C. (1972). Nonlocal polar elastic continua, *Int. J Eng. Sci.*, 10: 1–16.
- Eringen, A.C. (2002). *Nonlocal Continuum Field Theories*, Springer, New York.

Ghorbanpour Arani, A.; Haghparast, E.; Khoddami Maraghi, Z.; Amir, S. (2014). CNTRC Cylinder Under Non-axisymmetric Thermo-Mechanical Loads and Uniform Electromagnetic Fields. Arab J Sci. Eng., 39(12): 9057-9069.

Zenkour, A.M.; Arefi, M. (2017). Nonlocal transient electro-thermo-mechanical vibration and bending analysis of a functionally graded piezoelectric single-layered nanosheet rest on visco-Pasternak foundation. J. Therm. Stresses, 40 (2): 167-184.

AUTHOR (S) BIOSKETCHES

Ali Ghorbanpour Arani, Department of Chemical Engineering, College of Engineering, Shahid Bahonar University, Kerman, Iran, *Email: aghorban@kashanu.ac.ir*

Amir Hossein Soltan Arani, Department of Chemical Engineering, College of Engineering, Shahid Bahonar University, Kerman, Iran, *Email: soltanarani.ah@gmail.com*

Elham Haghparast, Department of Chemical Engineering, College of Engineering, Shahid Bahonar University, Kerman, Iran, *Email: elhm.haghparast@yahoo.com*